Hypoxia-induced Changes to Integrin α 3 Glycosylation Facilitate Invasion in Epidermoid Carcinoma Cell Line A431

Ren, Yan; Hao, Piliang; Law, Sai-Kit Alex; Sze, Siu Kwan

2014

Ren, Y., Hao, P., Law, S.-K. A., & Sze, S. K. (2014). Hypoxia-induced Changes to Integrin α 3 Glycosylation Facilitate Invasion in Epidermoid Carcinoma Cell Line A431. Molecular & Cellular Proteomics, 13(11), 3126-3137.

https://hdl.handle.net/10356/80751

https://doi.org/10.1074/mcp.M114.038505

To be submitted to *Molecular and Cellular Proteomics*

Hypoxia-induced changes to integrin alpha 3 glycosylation facilitate invasion in epidermoid carcinoma cell line A431

Yan Ren, Piliang Hao, S. K. Alex Law and Siu Kwan Sze*

School of Biological Sciences, Nanyang Technological University, 60 Nanyang Drive, Singapore 637551

Running title: Hypoxia inhibits ITGA3 glycosylation to speed cell invasion

Correspondence:
Siu Kwan SZE, PhD
School of Biological Sciences
Division of Structural Biology and Biochemistry
Nanyang Technological University,
60 Nanyang drive, Singapore 637551
Tel: (+65) 6514-1006
Fax: (+65) 6791-3856
Email: sksze@ntu.edu.sg

Abbreviations

Nx: normoxia; Hx: hypoxia; Reox: re-oxygenation; iTRAQ, isobaric tag for relative and absolute quantification; MRM, multiple reaction monitoring; LC-MS: Liquid chromatography–mass spectrometry; UFLC: ultra fast Liquid chromatography; HPLC: High-performance liquid chromatography; MDLC: Multi-dimensional liquid chromatography; ESI: Electrospray ionization; ERLIC: electrostatic repulsion hydrophilic interaction chromatography; HILIC: hydrophilic-interaction chromatography; FDR, false discovery rate; EF, error factor; PAGE, polyacrylamide gel electrophoresis; WB, Western blot; IP: immunoprecipitation; PCR, polymerase chain reaction; TCEP: tris-(2-carboxyethyl)phosphine; MMTS, methyl methanethiosulfonate; TEAB, triethylammonium bicarbonate; SDS: sodium dodecyl sulfate; DMEM, Dulbecco's modified Eagle's medium; PBS: Phosphate buffered saline; EDTA: ethylenediaminetetraacetic acid; FITC: fluorescein isothiocyanate; BSA: bovine serum albumin; FBS, fetal bovine serum; FN: fibronectin; IgG: Immunoglobulin G; FA, formic acid; ACN: acetonitrile; HIF-1, hypoxia-inducible factor-1; ECM, extracellular matrix; MMP, matrix metalloproteinase; ITGB1/4/6, integrin beta 1/4/6; ITGA2/3/5/6/V, integrin alpha 2/3/5/6/V; PTM: posttranslational modification; WT: wild type; 2D, Two-dimensional; MW: molecular weight; BCA: bicinchoninic acid assay; ATCC: American Type Culture Collection; ID: identity; ER: endoplasmic reticulum; NXS/T/C: Asparagine-(any amino acid except Proline)-Serine/Threonine/Cysteine; IDA: information-dependent acquisition; IR: ischemia and reperfusion;

Summary

Hypoxia is a critical microenvironmental factor that drives cancer progression through angiogenesis and metastasis. Glycoproteins, especially those on the plasma membrane, orchestrate this process; however, hypoxia-perturbed protein glycosylation in cancer cells remains unclear. We focused on the effects of hypoxia on the integrin family of glycoproteins, which are central to the cellular processes of attachment and migration and have been linked with cancer in humans. The ERLIC coupled with iTRAQ labeling and LC-MS/MS was employed to identify and quantify glycoproteins expressed in A431, which revealed that independent of its protein level change, N-glycosylation modifications of integrin alpha 3 (ITGA3) were inhibited by hypoxia, which was different from other integrin subunits. A combination of Western blot, flow cytometry and cell staining assays showed that hypoxia-induced alterations to ITGA3 glycosylation prevented its efficient translocation to the plasma membrane. Mutagenesis studies demonstrated that simultaneous mutation of glycosites 6 and 7 of ITGA3 prevented its accumulation at K562 cell surface, which blocked integrin alpha 3 and beta 1 heterodimer formation and thus abolished its interaction with extracellular ligands. By generating A431 cells stably expressing ITGA3 mutated at glycosites 6 and 7, we showed that lower levels of ITGA3 on the cell surface, as induced by hypoxia, conferred an increased invasive ability to cancer cells *in vitro* under hypoxic conditions. Taken together, these results revealed that ITGA3 translocation to the plasma membrane suppressed by hypoxia through inhibition of its glycosylation facilitated cell invasion in A431.

Key words: hypoxia, N-linked glycosylation, membrane ITGA3, invasion, A431

Introduction

As solid tumors grow, those areas distant from the existing blood vessels can become chronically or intermittently deprived of sufficient oxygen. These hypoxic conditions place tremendous pressure on tumor cells and drive development of increasingly malignant and metastatic phenotypes (1, 2). As metastases are responsible for over 90% of human cancer-related deaths, much research has aimed to define the underlying molecular mechanisms of the tumor cell response to a hypoxic microenvironment (3-5). However, despite the evident clinical relevance of metastasis, the full complexity of the process remains incompletely understood. An emerging area of interest is the importance of the carbohydrate structures in tumor cells, which have been linked to control of protein folding and stability, cell-cell recognition, adhesion, invasion, and metastatic potentials (6-11). The post-translational enzymatic addition of glycans (glycosylation) to proteins is a potent modulator of the functions of many receptors involved in cell growth, adhesion, and signal transduction (11-14), and is commonly seen in both *in vitro* and *in vivo* cancer models (15, 16). Furthermore, a growing body of studies has shown a clear correlation between aberrant glycosylation and human disease states, including cancers (11, 17, 18). Our previous proteomic and functional study revealed that glycosylation pathways in cell lines derived from human tumors are markedly altered by hypoxic conditions (5). Here we have gone on to investigate the significance of hypoxia-induced changes to glycosylation of specific proteins and to ask about the functional impacts of those changes in tumor cells with regard to the metastatic phenotype.

The process of metastasis can be broadly broken down into several steps that include detachment from the primary tumor mass, exit from tissues into the blood vessel, transport through the blood,

exit from the vessel at a distant site, and re-establishment in the new tissue(19). Central to the process is modulation of tumor cell adhesion to the extracellular matrix (ECM), other tumor or stromal cells, and the basement membrane - all of which involves members of the integrin family of adhesion molecules. Integrins are cell surface transmembrane glycoproteins that mediate cell-cell and cell-ECM attachment and communication, influencing cell cycle, motility, cytoskeletal organization and morphology(20). Appropriate regulation of the glycosylation of integrins is crucial for their biological functions: for example, integrin α6β1 could not bind to its ligands or be normally transported to the cell surface after treatment of cells with tunicamycin, a glycosylation inhibitor (21); and cleavage of the N-glycans of purified integrin α5β1 blocked both heterodimer formation and ligand interaction (22). Aberrant changes in the N-glycosylation of integrins are often seen during carcinogenesis and have profound downstream effects on cell spreading and migration (23-25), both of which could feasibly impact metastatic potential of tumor cells. Functional integrin heterodimers comprise large (α) and small (β) subunits. In mammals, eighteen α and eight β subunits have been characterized, which combine to generate 24 unique integrin heterodimers (26). Multiple integrin subunits are upregulated under hypoxic conditions in a range of cell types (5, 27, 28). Of these, integrin α3β1 is an enigmatic member of the integrin family and the regulation of its function also marks it as distinct from that of other integrins (29). It was originally identified as a promiscuous receptor for a range of ligands including collagen, laminin-1, fibronectin and entactin (30, 31), but has since been shown to favor laminin-5 and a5-containing laminins as ligands (32, 33), and perhaps thrombospondin-1 in certain cell types (34). There is much interest in the possible role of integrin α3β1 in migration and metastasis of tumor cells (35). Early studies linked decreased expression of integrin α3β1 with the malignant phenotype in breast and lung cancer cells (36, 37), and more recently it was

shown that expression of integrin α3β1 was downregulated in transformed cells overexpressing the transcription factors c-myc or n-myc (38, 39). Other investigators suggested that integrin α3β1 might also stimulate invasiveness in certain tumors, particularly non-epithelial types that expressed laminin-5 (40, 41). Our own data showed that the overall protein expression level of ITGA3 was slightly induced by hypoxia in A431 (5); however, the changes of its glycosylation and thus its effect on cell migration remain unstudied under hypoxia.

Considerable technical challenges exist for the accurate study of glycosylated proteins in complex biological systems, and to date several approaches have met with some success. The most commonly employed technique for the analysis of protein glycosylation is HPLC coupled to MS (42, 43). A number of HPLC protocols have been developed which enable the enrichment of glycopeptides from complex samples, including lectin affinity (44, 45), hydrazide reaction (46), ion-exchange (47), hydrophilic-interaction chromatography (HILIC)(48), and TiO2 (49). For quantitative analysis of glycoproteins, Zhou et al. analyzed N-glycoprotein profiles in tear fluid using hydrazide-resin capture, iTRAQ labeling and 2D-LC-MS/MS identification: a total of 43 unique N-glycoproteins were identified and some were found to be modulated at several glycosites under disease conditions (50). In 2012, Palmisano et al. quantified formerly *N*-linked sialylated glycopeptides by TiO_2 and salt-free fractionation with HILIC for enrichment, finding that 300 unique sialylated glycopeptides were regulated during mouse brain development (51). Recently, the development of electrostatic repulsion hydrophilic interaction chromatography (ERLIC), a mixed-mode chromatography technique, has enabled glycopeptide and phosphopeptide enrichment based on both their electrostatic and hydrophilic properties, which

permits identification of glycoproteins from complex mixture by chromatographic enrichment and has been proved compatible with iTRAQ labeling (52-55).

We believed that application of these techniques to the quantitative assessment of protein glycosylation in cancer cells would lead to substantial advances in our understanding of the biology of human tumor cells. Therefore, in this study we employed ERLIC to enrich glycopeptides from tumor cell lysates coupled with iTRAQ labeling and LC-MS/MS for identification and quantification of N-glycosylated peptides. N-glycosylation modification of ITGA3 was detected downregulated and thus blocked its secretion to plasma membrane under hypoxia, which was confirmed to enhance A431 cell invasion.

Experimental Procedures

Chemicals and reagents

Reagents were purchased from Sigma Chemical Co. (St. Louis, MO) unless otherwise specified. Antibody against ITGA3 for WB and cell staining was from Proteintech (Chicago, IL) and BioLegend (San Diego, CA), respectively. The FITC-conjugated anti-ITGA3 and isotope control for flow cytometry was from AbD Serotec (Toronto, Ontario Canada). Anti-actin (clone C4 | MAB1501) and anti- ITGB1 were purchased from Millipore (Billerica, MA) and Santa Cruz (Santa Cruz, CA), respectively. Human Laminin 5 was from Abcam (Cambridge, UK). Hygromycin B was bought from PAA Laboratories (Piscataway, NJ). EZ-Link Sulfo-NHS-LC-Biotin and avidin were purchased from Thermo Scientific (Rockford, IL). PNGase F was ordered from New England Biolabs (Ipswich, MA). Protease inhibitor cocktail tablets were obtained from Roche (Basel, Switzerland).

Cell culture and hypoxic conditions

The A431 human epithelial carcinoma cell line was purchased from ATCC and maintained in DMEM with 10% FBS. Nomorxia, hypoxia and re-oxygenation treatments of A431 were performed as described previously (4, 5). Briefly, the cells cultured in serum free media were exposed to Normoxia (Nx: 21% O_2, 5% CO_2) in a normal incubator or hypoxia (Hx: <0.1% O_2, 5% CO_2) in a modular incubator chamber (Billups-Rothenberg Inc. Del Mar, CA). For Re-oxygenation (Reox), the cells were exposed to Nx after a period of Hx culture and accompanied with changing into fresh media. At least three independent biological replicates were pooled for the analyzed samples in each condition. The human chronic myelogenous leukemia cell line K562 was from ATCC and maintained in RPMI 1640 with 10% FBS.

Sample preparation, glycopeptide enrichment, iTRAQ labeling, and LC-MS/MS analysis

We employed an integrated strategy to allow identification and quantification of glycoproteins in human cancer cell lines exposed to a range of oxygenation conditions (Fig. 1). Firstly we used ERLIC to enrich glycopeptides from the total tryptic peptides from A431 that had been subjected to Nx (72h), Hx (48h or 72h) or Hx (48h)/Reox (24h). The enriched glycopeptides were then treated by PNGase F to remove their N-glycans followed by labeling with iTRAQ reagents. These labeled deglyco-peptides were fractionated by ERLIC again and then identified and quantified by Q-Star Elite MS because ERLIC has been proved as a more convenient and more effective alternative to SCX for the fractionation of iTRAQ-labeled peptides(55).

Nonenzymatic deamidation occurs in peptides under basic conditions commonly used in treatment with trypsin and PNGase F. Our previously published results showed that digesting peptides in pH 6.0 and releasing glycans in pH 5.0 significantly reduced the artifacts of glycosite identification from deamidated peptides introduced in sample preparation(56). The solutions with pH 6.0 and with pH 5.0 were used to extract A431 proteins and remove glycans of peptides after enrichment, respectively. Cellular proteins were extracted by 8M urea in 20 mM phosphate buffer (pH 6) solution with protease inhibitor cocktail (1:50). 4mg of proteins from cells exposed to each oxygenation condition were reduced, alkylated and digested by trypsin as described previously (5). For glycopeptide enrichment, the peptides were suspended in 80% ACN with 0.1% FA and passed through an ERLIC column (PolyLC, Columbia, MD; 4.6 ×200 mm, 5μm particle size, 300-Å pore size) with a 78min gradient at 0.5ml/min flow rate, as per our previous research (0% buffer B for 10 min, 0-8% buffer B for 20 min, 8-12% buffer B for 6 min and 100% buffer B for 42 min; A: 80% ACN/0.1% FA; B: 10% ACN/2% FA)(52). The peptides from the 36-78min gradient were pooled and dried for deglycosylation. Phosphate buffer (pH 5) was used to dissolve the glycopeptides and for releasing N-linked glycans by PNGase F according to its instruction manual. The peptides without glycans were dissolved in 1M TEAB (pH 8.5) and labeled with the isobaric tags (Applied Biosystems, Foster City, CA) according to manufacturer's protocol as following: the Nx-treated sample was labeled with 114; the samples under Hx for 48 hr or 72 hr were labeled with 115 and 116 respectively; and the ReOx-treated sample was labeled with 117.

The labeled sample was fractionated on an ERLIC column (PolyLC, Columbia, MD; 4.6 ×200 mm, 5μm particle size, 300-Å pore size) again using Shimadzu Prominence UFLC system (Kyoto, Japan). Fractionation was performed with a 60-min gradient at a flow rate of 0.9 ml/min

(0% buffer B 5 min, 0_28% buffer B for 40 min, 28_100% buffer B for 5 min and 100% buffer B for 10 min; A:10 mM CH3COONH4 in 85% ACN/1% FA; B: 30% ACN/0.1% FA). A total of 30 fractions was collected and desalted using Sep-Pak C18 cartridges. Each fraction was dried and reconstituted in 40µl 3% ACN and 0.1% formic acid for Q-Star Elite LC-MS/MS analysis as previously described (4, 5). Briefly, peptides were separated on a home-packed nanobored C18 column with a picofrit nanospray tip (75µm inner diameter×15 cm, 5µm particles) (New Objectives, Woburn, MA) in a flow rate of 300 nL/min with 90min gradient (13_15%B for 1min, 15_23%B for 14min, 23_40%B for 55min, 40_65%B for 5min, 65_90%B for 3min, 90%B for 2min, 90_13% B for 1min and 13%B for 9min; A: 0.1% FA and B: 80% ACN in 0.1% FA). MS data was acquired in positive ion mode with a mass range of 300-1600 m/z using Analyst QS 2.0 software (Applied Biosystems). Peptides with +2 to +4 charge states were selected for MS/MS. The three most abundance peptides were selected for MS/MS and dynamically excluded for 30 s with a mass tolerance of 0.03 Da. The peak areas of the iTRAQ reporter ions were used to quantify proteins in the samples.

Database searching and criteria

Protein identification and quantification were performed using ProteinPilot^{TM} software 3.0 with Revision number 114732 (Applied Biosystems) by searching the combined raw data from the two runs of labeled sample against the concatenated “target” (Uniprot human database, downloaded on 14 June 2012, including 87187 sequences) databases. The Paragon and Pro Group algorithms in the ProteinPilot software were used for peptide identification and isoform-specific quantification. User-defined parameters were as follows: (i) sample type, iTRAQ 4plex (peptide-labeled); (ii) cysteine alkylation, MMTS; (iii) digestion, trypsin; (iv) instrument, QStar

Elite ESI; (v) special factors, emphasis on N deamidation; (vi) species, none; (vii) specify processing, quantitative; (viii) ID focus, biological modifications; and (ix) search effort, thorough ID. The resulting data were automatically bias-corrected to account for potential reporter variations due to the possible unequal quantities of proteins in the different labeled samples. During bias correction, the software identifies the median average protein ratio and corrects it to unity, and then applies this factor to all quantitation results. For iTRAQ quantitation, the peptide for quantification was automatically selected by the Pro Group algorithm to calculate the reporter peak area, error factor (EF), and p value.

Glycopeptide identification and quantitation

Only the peptides with identification confidence≥95 % were adopted as identification. The glycopeptides were picked up according to the motif of NXS/T/C (X is any amino acid except P) with deamidation of N to D. To evaluate the identified glycosites, they were matched with the glycosites annotated in Uniprot database by our in-house perl program. The results contained the information of glycosite position in the amino acid sequence and which type annotation of the glycosite in Uniprot database (with reference support, potential or unknown). The ratio of glycosites with 'unknown' or 'with reference support' partially indicated the quality of glycosite identification. To further confirm the quality of identification, manual check for spectrum of each glycopeptide was performed. Sometimes database searches can return some false-positive identification of deamidated peptides because the ^{13}C peaks of amidated peptides can be wrongly assigned as the monoisotopic peaks of the corresponding deamidated peptides(56). The close N or Q to the motif of glycosylation can also cause false-positive identification if the evidences are not enough to confirm which one is really deamidated.

For quantification, only the glycopeptides with less than 20% area error were adopted. The mean±SD of quantification ratio for all identified glycopeptides from the same protein was calculated as its fold change. For individual glycopeptide, its fold change was calculated by its all quantification from different scans. The paired t-test was used for statistical analysis between two groups. Significance level was set at $p<0.05$.

Cell membrane fractionation by ultracentrifugation

Cell membrane purification was performed as described previously (53), with minor modifications: cells were collected by centrifugation at 4°C, suspended in HES buffer (20 mM HEPES, pH 7.4, 1 mM EDTA, 250 mM sucrose) supplemented with protease inhibitor (Roche Diagnostics) and homogenized by repeated passage through a 27-gauge needle until most of the cells were lysed with intact nuclei released. The nuclei, remaining debris and unbroken cells were removed by centrifugation at 1000×g for 10 min at 4°C. Resulting supernatants were transferred to an ultracentrifuge tube and centrifuged at 100,000×g for 1h at 4°C. The pellets containing membrane fractions were re-suspended in Na_2CO_3 (0.1 M, pH 11) and sonicated for 30sec on ice followed by centrifugation at 100,000×g for 1 h at 4°C. After washing twice with Milli-Q water, membranes were collected by centrifugation at 100,000×g for 30 min at 4°C. The membrane pellet was then dissolved in 8 M urea solution, and protein content was determined with a 2-D Quant kit (GE Healthcare) according to the manufacturer's instructions.

Cell surface biotinylation

K562 cells were washed three times with ice-cold PBS (pH 8.0) to remove amine-containing medium and proteins from the collected cells. The cells were then suspended at a concentration

of ~25×10^6 cells/ml in PBS (pH 8.0). Freshly-prepared 10mM Sulfo NHS-LC-Biotin reagent was added (200µL/mL cell suspension) and incubated with the cells at room temperature for 30 min. Finally the cells were washed three times with ice-cold PBS with 25mM Tris-HCl to remove and quench excess biotin-labeling reagent and its by-products. The biotinylated cells were then exposed to lysis buffer (20mM Tris-HCl, pH 7.4, 150mM NaCl, 1% Triton X-100, Complete™ EDTA-free protease inhibitor mixture) before incubation with avidin at room temperature for 1h. After washing the beads with lysis buffer 3 times, reducing SDS-PAGE loading buffer was used to elute the biotinylated proteins for WB as described below.

Cell labeling for microscopy and flow cytometry

For microscopy, A431 cells were stained with anti-ITGA3 (1:50, BioLegend) as described before (5). For flow cytometry, collected cells were washed three times with ice-cold PBS then incubated with 5% human serum in PBS for 30min on ice for blocking. Isotype control antibody (negative control) or FITC-conjugated anti-ITGA3 antibody was added and incubated for 1h on ice. After washing three times with 1%BSA in PBS, flow cytometry analyses were performed using a FACSCalibur instrument (BD Biosciences) operated with CELLQuestPro software.

Release of N-glycans from glycoproteins in solution

N48 and H48 A431 cell proteins were extracted in lysis buffer (1% SDS, 50mM Tris-HCl, pH 8). The proteins with 0.5% SDS were denatured under 100°C for 10min in 40mM DTT. After cooling, PNGase F (1:200. v/w) was added into the denatured proteins in 1×G7 buffer with 1% NP-40 (supplied with PNGase F kit). The reaction was stopped with heating 100°C for 10min after incubation at 37°C for 6h. 20µg total proteins were used for WB.

Immunoprecipitation and Western blotting

Cells were washed three times with ice-cold PBS before addition of lysis buffer (20mM Tris-HCl, pH 7.4, 150mM NaCl, 1% Triton X-100, Complete™ EDTA-free protease inhibitor mixture). 31G needles were used to facilitate cell lysis. The cell lysates were centrifuged at 12,000×g for 15min at 4°C. The supernatants were collected and incubated with 3µL ITGA3 antibody overnight and then 15 µL of protein G-Sepharose was added for a further 1h at 4°C. After washing with lysis buffer 3 times, SDS-PAGE loading buffer was used to elute proteins from the sepharose beads for WB. The complexes were resolved by 7% SDS-PAGE and then transferred to nitrocellulose membrane and immunoblotted using antibodies as indicated in the figures. Proteins of interest were detected using the Invitrogen ECL system according to the manufacturer's instructions. For general WB, protein concentration of cell lysates dissolved in 1% SDS in 40mM Tris-HCl (pH 8.0) was quantified using BCA assay to enable equal total protein amounts from each sample to be used for comparison.

Construction and mutagenesis of ITGA3 expression vectors

Full length ITGA3 cDNA was obtained from the A431 cDNA library by PCR as mentioned before (5). There are two isoforms of ITGA3 in mammalian cells: isoform 1 is widely expressed while isoform 2 is expressed only in brain and heart. Thus we designed primers for the common isoform 1 of ITGA3 (Supplemental Table S4). The ITGA3 gene was inserted into the expression vector pCDNA3.1+/Hygromycin. For mutagenesis, the primers were designed by the software of QuickChange Primer Design from Agilent Technologies (http://www.genomics.agilent.com/primerDesignProgram.jsp) (Supplemental Table S5). The

mutations of glycosites within ITGA3 were performed using QuikChange II Site-Directed Mutagenesis Kit (Agilent Technologies) according to the manufacturer's protocol. All sequences of WT-ITGA3 and its mutants were confirmed by DNA sequencing. For stable expression of WT or mutated ITGA3, K562 and A431 cells were transfected using lipofectamine 2000 (Invitrogen) at a ratio of 1:5(w/w) according to the manufacturer's instructions. Successfully transfected cells were then selected by culturing in standard medium with 0.4mg/ml hygromycin B. After two weeks, to get monoclones with WT or mutated ITGA3 expression in K562, the cells were diluted into at most one cell/well in 96 well plates. For A431 monoclones, they were picked up from the plates by trypsin digestion. The positive clones were confirmed by WB.

Knockdown of ITGA3 expression in A431

The primer sequences for shRNA knockdown of ITGA3 or luciferase (control) were generated by the Invitrogen BLOCK-iT™ RNAi Designer (Supplemental Table S5). These fragments were then inserted into shRNA vector pSuperior-retro-puro after annealing according to the manufacturer's instructions. The shRNA plasmids with positive insertions were transfected into A431 by lipofectamin 2000 (Invitrogen) following the manufacturer's protocol. Cells were then selected with standard medium with 0.5ug/ml puromycin. After one week, the monoclones were picked up from the plates by trypsin digestion. The positive clones were confirmed by WB.

Cell spreading assay

96-well plates were either coated with 2 μg/mL laminin 5, or 0.5 % BSA in DMEM as a negative control. K562 cells were seeded at 5 x 10^4 live cells per well and incubated for indicated time at 37°C before imaging at 100 × magnification by light microscopy. To assess spreading of K562

cells on an *in vitro* ECM, A431 cells were cultured on glass coverslips for 3-5 days before removal by sequential washing with 1% Triton X-100 in PBS, 2M urea in 1M NaCl and 8M urea (all containing protease inhibitor cocktail). The resulting coverslips were washed with PBS, blocked with BSA and used in cell spreading assays (32).

Transwell invasion assay

24-well Transwell plates containing 8-μm-pore size polycarbonate filters (Corning Costar, Cambridge, MA) were used for invasion assay. Transwell insert membranes were coated with 100 μl of laminin 5 and incubated overnight at 4 °C. Triplicate was performed for each cell line. 4×10^4 cells in 100 μl serum-free medium were seeded in each top Transwell insert and 600 μl media with serum were added in lower chamber. After incubated for 24h, the cells without migration were swabbed from upper well using cotton buds. Cells that had migrated through the membranes were fixed with 4% formaldehyde for 20 minutes and then stained with the crystal violet for image capture and counted under a light microscope. For quantification, the membranes were cut carefully from inserts. The cells on them were solubilized by 200 μl of 0.5% Triton X-100 overnight at room temperature. The absorbance was measured at A_{595} using a microplate reader (Tecan Magellan, Männedorf, Switzerland).

Statistical analysis

Values are expressed as mean±SD. The paired t-test was used for statistical analysis between two groups. Significance level was set at $p<0.05$.

Results and Discussion

Analysis of identified glycoproteins enriched by ERLIC

Protein and peptide identification summary results were listed in Supplemental Tables S1 and S2. A total of 1209 proteins were identified with at least 2 unique peptides (Confidence ≥95%). For glycopeptides, only those with confidence ≥95% were adopted as identification and used for further analysis. Glycopeptides were detected by possession of the motif NXS/T/C (where X is any amino acid except P and N is deamidated). In total, 241 glycopeptides with 215 glycosites were identified, belonging to 146 proteins. Matching these glycosites with those provided in Uniprot database, we found that 93 glycosites already had 'Reference support', and 50 sites were classified as 'potential' and only 72 (33.5%) were 'unknown'(Table 1 and Supplemental Table S3_1-3). Putative false positive N-glycosites were highlighted by matching with the potential false N-glycosites obtained from A431 whole proteome analysis, in which the proteins were digested at pH 8.0 without PNGase F treatment. Altogether 26 glycosites in this study were also identified in the whole proteome analysis, with 24 of these in the 'unknown' group and 2 in 'Reference support'. The deamidation of asparagine is accelerated when the following amino acid is glycine, which can easily cause false positive glycosylation identification during sample preparation (57), and accordingly 12 of these deamidated N peptides (46.2%) were in N-G-S/T sequences (Supplemental Table S3_1-3). To further confirm the identification, the MS/MS spectra of peptides with putative N-glycosites identification were checked manually one by one. In total, 180 spectra with fragmentation matching evidence were provided with higher confidence including all the 93 glycosites with Uniprot 'Reference support', 48 of 50 Uniprot 'potential' sites and 39 of 72 Uniprot 'unknown' sites (Supplemental Table S3_1-3). The

Functional Annotation Clustering tool from DAVID Bioinformatics Resources 6.7 (http://david.abcc.ncifcrf.gov/tools.jsp) was used to group the 146 proteins (58). It indicated that 101 of the 146 proteins we identified with N-glycosites were known N-linked glycoproteins, with 84 of these being membrane-associated, 70 of which belonging to the plasma membrane. The dominant functional category was cell adhesion (Supplemental Figure S1). As a major family of adhesion proteins, integrins play an important role in cell adhesion and migration. Accordingly the pathway analysis of the 146 proteins using Panther classification system (http://www.pantherdb.org) revealed that integrin signaling pathway was also the dominant category (Figure 2A). Within the integrin category we identified 7 integrin subunits, and quantified the glycopeptides of these subunits that were modulated by hypoxia and re-oxygenation (Supplemental Table S4 and Figure 2B). Only 5 integrin subunit quantification information was presented in Figure 2B because ITGA6 and ITGB6 had no statistical quantification information to represent their changes due to hypoxia (Supplemental Table S4). For hypoxia 72h, all the five integrin subunits had an increase in glycosylation with $p<0.005$, in which ITGA3 had a slightest increase with a ratio of 1.11±0.2 and the others had a ratio more than 1.3. The quantification results were consistent with our findings in A431 whole proteome analysis for hypoxia 72h (ITGA3: 1.14±0.21) (5). Interestingly, for hypoxia 48h, only ITGA3 had a significant decrease in glycosylation modification with $p<0.005$ (0.82±0.12). The integrin quantification results were confirmed by a new iTRAQ analysis with 2 MS running in another biological repeat: ITGA3 downregulated at H48 (0.9±0.22) and slightly upregulated at H72 (1.17±0.26) (Supplemental Table S4). Our previous study showed that the total protein expression level of integrin subunits (ITGA5/3/6/V, ITGB1/4) under hypoxia was up-regulated (5), and therefore the increased level of glycosylated integrin subunits found here (ITGA5/2/V

and ITGB1) might have been attributed to their whole expression level upregulation; however, the level of glycosylated ITGA3 decreased under H48 where its total protein level increased (ITGA3: 1.14±0.12 and 1.15±0.09 for iTRAQ and LC-MRM-MS/MS, respectively). Three glycosites of ITGA3 (glycosite 1/7/13) were identified in our iTRAQ data; Figure 2C indicated that all the three sites were significantly less glycosylated ($p<0.05$) under hypoxia 48h. In 2011, Parker et al. enriched and quantified the iTRAQ labeled N-glycopeptides during myocardial ischemia and reperfusion (I/R) injury by a sequential enrichment with TiO2 followed by IPZIC-HILIC for the unbound fraction. More than 400 N-linked glycopeptides were statistically quantified and 80 glycosylation sites were found altered, in which the glycosylation of several integrin subunits (ITGA6/7/V and ITGB1) were also found upregulated following I/R injury (59). They were consistent with our findings.

Translocation of ITGA3 to the plasma membrane was suppressed under hypoxia

Western blot (WB) was performed to confirm the levels of ITGA3 protein in lysates from A431 cells under normoxia, hypoxia and re-oxygenation conditions. As shown in Figure 3A, two different MW isoforms of ITGA3 were detected: the abundance of the lower MW isoform appeared no significant changes induced by hypoxia, while the higher MW isoform seemed to decrease obviously after hypoxia 48h and slightly after 72h, with clear recovery of expression level upon re-oxygenation. These results clearly showed that the real changes in abundance of the higher MW ITGA3 isoform were identified by glycopeptide quantification; whereas they had been obscured by the relatively more abundant low MW isoform in our previous whole proteome quantification(5). Because ITGA3 undergoes extensive glycosylation in the ER and Golgi during translocation to the plasma membrane, we hypothesized that the higher MW ITGA3 isoform

would be destined to the plasma membrane and therefore more relevant for tumor cell attachment and migration. To prove our hypothesis, PNGase F was adopted to treat the cell proteins from normoxia and hypoxia. Figure 3B revealed that both ITGA3 isoforms disappeared and combined as one band with lower MW after PNGase F treatment to remove N-glycans. This result clearly indicated that both of them had glycosylation modifications and the higher MW isoform had more glycosylation than the lower one. Membrane fraction WB result confirmed that the decrease in the higher MW ITGA3 isoform in response to hypoxia was more pronounced in plasma membrane fractions than that in whole cell lysates (Fig. 3A lowest panel). Whole A431 cells exposed to the different oxygenation conditions were then surface labeled with ITGA3-specific FITC-conjugated antibodies and the intensity of ITGA3 expression at the cell surface was quantified by flow cytometry. The results further confirmed that less membrane ITGA3 was present following 72h of hypoxia compared to normoxia for 72h. In agreement with the WB results, membrane ITGA3 levels recovered in the cells undergoing 24h re-oxygenation after 48h hypoxia treatment (Fig. 3B). The decrease of membrane ITGA3 in cell staining was also observed by fluorescence microscopy (Fig. 3C). Thus, though hypoxia does not markedly affect the overall expression level of ITGA3 in A431 cells, it decreases ITGA3 glycosylation which is associated with lower abundance of ITGA3 at the plasma membrane.

N-linked glycosylation at sites 6 and 7 are essential for the translocation of ITGA3 to the plasma membrane.

To study the functional impacts of the changes to ITGA3 glycosylation induced by hypoxia, we first constructed a stable cell line expressing either WT ITGA3, or ITGA3 mutated at its potential glycosites. K562 cells do not express ITGA3 but do express its binding partner ITGB1

(60, 61), which renders them a good model for measuring changes in the biological function of ITGA3 following heterodimerization to form the active α3β1 integrin receptor. The 14 potential N-glycosylation sites of human ITGA3 are: (Asn-Xaa-Ser/Thr), Asn-86, Asn-107, Asn-265, Asn-500, Asn-511, Asn-573, Asn-605, Asn-656, Asn-697, Asn-841, Asn-857, Asn-926, Asn-935, and Asn-969, which are all located in the extracellular segment. We constructed 9 potential N-glycosite mutants as shown in Supplemental Figure S2; those sites within the β–propeller domain were chosen as mutation targets following the report that glycosites in this domain were required for membrane translocation of another integrin family member ITGA5 (9). All primers for ITGA3 expression and mutation are listed in Supplemental Table S5. The pcDNA3.1+/Hygromycin plasmids containing WT or mutated ITGA3 sequences were transfected into K562 cells. Surface ITGA3 expression was measured on transfected cells by flow cytometry. Supplemental Figure S3 shows that some cell sub-populations with membrane ITGA3 were detected in the pool of cells transfected with WT, M6, M7 and M3-5 -containing plasmids, but cells expressing M6-7 had no membrane ITGA3. Membrane ITGA3 was also detected on M3/4/5-transfected cells (data not shown). This suggested that the secretion of ITGA3 might be blocked by the simultaneous mutation of glycosites 6 and 7. To confirm this conclusion, two WT ITGA3-positive clones and two M6-7-ITGA3-expressing clones were selected for more detailed analysis. As shown in Figure 4A, WB revealed that the WT ITGA3 clones expressed both the higher and lower MW isoforms of ITGA3, as in A431 cells; however, the M6-7 clones expressed only one lower MW form of ITGA3, consistent with less glycosylation. From this we hypothesized that M6-7 ITGA3 would be absent on the plasma membrane because it might not complete intact glycosylation modification through Golgi to form the isoform with higher MW, and this was confirmed by WB of membrane fractions of the

transfected cells. No membrane ITGA3 bands were detected in the two clones of M6-7, but two bands were developed in the membrane fractions of WT clones with more enrichment for the bigger isoforms. The WB results from biotin-labeled fractions of membrane surface proteins further confirmed the lack of membrane ITGA3 in the two M6-7 expressing cell lines. In this result, mainly the bands with lower MW in WT cell lines were detected after enrichment and the higher bands were developed with over exposure after loading more samples (data not shown). It is possible that the biotin reagent (EZ-Link Sulfo-NHS-LC-Biotin) only reacts efficiently with primary amines exposed on surface, but the primary amines in the isofoms with higher glycosylation are blocked by glycans, which causes inefficient labeling finally. The IP results similarly showed an absence of membrane ITGA3 in the cell lines of clones expressing M6-7-mutated ITGA3: using an IP antibody recognizing the C-terminus of ITGA3 we found that only ITGB1 was detected in WT ITGA3 IP products and no ITGB1 was bound with M6-7 ITGA3 in its IP products, even with more M6-7 ITGA3 precipitation. The impact of the absence of ITGA3-B1 heterodimers on the cell membrane was then functionally assessed in a cell spreading assay. As expected, transfection of WT ITGA3 enabled rapid K562 cell adhesion and spreading onto plates coated with the α3β1 ligand Laminin 5 within 20 min (Fig. 4B), which was abolished by the addition of an anti-ITGA3 antibody, but not by normal mouse IgG (data not shown). In contrast, expression of the ITGA3 glycosylation mutant M6-7 did not rescue cell spreading even cultured for more than 2 hours on the plates coated with laminin 5. On the other hand, the transfection of M3-5 did induce cell attachment and spreading on laminin 5-coated plates, as did overexpression of the WT ITGA3 in K562 cells (data not shown). The same pattern of results was observed on plates coated with A431-derived ECM (data not shown). Together these results suggest that N-glycosylation at sites 6 and 7 in the ITGA3 subunit is essential for its

translocation to the cell surface and its biological functions. In ER, newly synthesized ITGA3 precursors undergo N-glycosylation and folding facilitated by the chaperone calnexin, which are assembled with ITGB1 and other proteins as a complex. The proper folded and assembled complex is then transported to the Golgi, where its high mannose glycans are processed to complex types and mature integrin α3β1 is formed finally. The lack of glycosylation at sites 6 and 7 might cause a failure to reach the final conformation for the complex formation and thus prevent the traffic of ITGA3 to plasma membrane. Nicolaou et al. reported that gain of glycosylation at a.a. 349 of ITGA3 by mutation impeded its heterodimerization with ITGB1 and thus impaired its expression at the cell surface, which provided a strong support to explain the impacts of ITGA3 conformation on its traffic and functions(11). The molecular mechanism that controls specific site glycosylation still remains unclear. Our tries to prove that the glycosylation of sites 6 and 7 was reduced simutaneously due to hypoxia failed so far. The partners that favor integrin α3β1 complex assembling might be good targets for hypoxia regulation to control ITGA3 transport process.

Decreased surface ITGA3 enables increased A431 cell migration under hypoxic conditions

The integrin α3β1 is important for cell migration, but both positive and negative effects have been reported (62-64), with one study even finding that knockdown of ITGA3 in keratinocytes compromised collective migration, but enhanced single cell migration (65). To mimic the changes in ITGA3 induced by hypoxia, the cDNAs of WT and mutants were transfected into A431 to find the impacts of less membrane ITGA3 on cell invasion. As shown in Figure 5A, WB of lysates from A431-WT cells had the same two bands as the control-plasmid transfected cells, but a marked increase in expression of the higher MW isoform. A431-M3-5 cell lysates had four

bands; two for the original WT ITGA3 isoforms basally expressed by A431 and two lower isoforms following original ones arising from partially glycosylated M3-5 ITGA3 mutants. A431-M6-7 produced only three bands; two for basal WT ITGA3 expression, and the third with lower MW representing expression of the less glycosylated M6-7 ITGA3. This phenomenon was consistent with the expression of WT and mutant ITGA3s in K562. Moreover, it seems that the overexpression of WT and M3-5 causes a greater increase in ITGA3 isoforms with higher MW than that of lower isoforms. The membrane ITGA3 in each stable cell line was detected by flow cytometry. In Figure 5B, it is clear that WT and M3-5 belong to the same population with similar membrane ITGA3 expression, which has higher membrane ITGA3 than the population of control and M6-7. The functional effects of different ITGA3 expression in the cells were then evaluated by transwell invasion assay with human laminin 5 coating under normoxic conditions for 24h. Markedly, much more trans-membrane was observed in cells overexpressing WT (2.5±0.2 fold) or M3-5 (3.1±0.1 fold) ITGA3, compared with control cells transfected with pcDNA3.1+ (Figure 5C). Under normoxic conditions A431-M6-7 cells exhibited similar invasive ability to the control cells, in accordance with their similar membrane levels of ITGA3 (Figure 5B and 5C). It has been reported that integrin α3β1 promotes radiation-induced migration of meningioma cells and suppression of integrin α3β1 inhibits tumorigenesis and invasion in breast cancer cells (66). Our transwell assay on the ITGA3 knockdown cells also supported the same conclusion. Less total and membrane ITGA3 expression in A431 suppressed cell invasion through laminin 5 coated membranes under normoxia (Supplemental Figure S4). In contrast, the transwell invasion assay performed under hypoxia revealed that the invasion of cells with WT and M3-5 overexpression was substantially less than that of control cells (0.41±0.02 and 0.59±0.01) while cells transfected with the M6-7 mutant had a higher relative invasion rate (0.75±0.02 of control

cells) compared with WT or M3-5 overexpression cells (Figure 5D). In these assays, M3-5 had similar invasive ability with WT because it had normal membrane secretion of ITGA3 even with 3 glycosite mutation. For M6-7, it had similar behavior with control cells due to lack of membrane ITGA3. These transwell invasion assay results clearly showed that under normoxia the extent of cell invasion positively correlated with the level of plasma membrane ITGA3 whatever in ITGA3 overexpression or knockdown A431 cells. Under hypoxia, however, the situation was different; A431-WT transfected cells, with higher levels of plasma membrane ITGA3, had a lower invasion than A431-M6-7 with less plasma membrane ITGA3. Thus we conclude that less ITGA3 translocation to the cell membrane, as induced by hypoxia, increase invasion of A431 cells in sub-optimal oxygenation conditions.

Conclusions

In this study, we quantified N-glycoproteins from normoxic, hypoxic and re-oxygenated A431 cells using iTRAQ-based proteomic approaches. Taking into account the clinical significance of metastasis, we focused on the integrin family of cell adhesion molecules and in particular ITGA3. We detected substantially decreased levels of N-glycosylated ITGA3 under hypoxia, which were independent of changes in its protein level. We showed that specific glycosylation sites within ITGA3 were required for its normal trafficking to the cell surface, and so its dimerization with ITGB1 and functional effects. Thus we have revealed a new pathway through which hypoxia can potentially modulate tumor cell behavior in order to favor metastasis. More broadly, this study highlights the power of glycoproteomics to enrich the data generated by more conventional proteomic studies and to elucidate the true functional significance of modulations to glycoproteins in both health and disease states.

In addition, it is an intriguing question to find why simultaneous mutations of glycosites 6 and 7 cause ITGA3 deficient in plasma membrane. The conformation changes due to lack of glycans on sites 6 and 7 should be the keys to open the mysterious doors to reveal the interaction of integrin α3β1 complex. It is our future work to find ITGA3 partners which help its traffic to plasma membrane and confirm whether these partners are downregulated by hypoxia in A431. It could give clues for underlying mechanism behind metastatic cascades and provide new insights in the studies on cancer cell hypoxia.

ACKNOWLEDGEMENT

This work is supported by the Singapore Ministry of Health's National Medical Research Council (NMRC/CBRG/0004/2012).

References

1. Subarsky, P., and Hill, R. P. (2003) The hypoxic tumour microenvironment and metastatic progression. *Clin Exp Metastasis* 20, 237-250.
2. Majmundar, A. J., Wong, W. J., and Simon, M. C. (2010) Hypoxia-inducible factors and the response to hypoxic stress. *Mol Cell* 40, 294-309.
3. Tsai, Y. P., and Wu, K. J. (2012) Hypoxia-regulated target genes implicated in tumor metastasis. *J Biomed Sci* 19, 102.
4. Park, J. E., Tan, H. S., Datta, A., Lai, R. C., Zhang, H., Meng, W., Lim, S. K., and Sze, S. K. (2010) Hypoxic tumor cell modulates its microenvironment to enhance angiogenic and metastatic potential by secretion of proteins and exosomes. *Mol Cell Proteomics* 9, 1085-1099.
5. Ren, Y., Hao, P., Dutta, B., Cheow, E. S., Sim, K. H., Gan, C. S., Lim, S. K., and Sze, S. K. (2013) Hypoxia modulates A431 cellular pathways association to tumor radioresistance and enhanced migration revealed by comprehensive proteomic and functional studies. *Mol Cell Proteomics* 12, 485-498.
6. Varki, A. (1993) Biological roles of oligosaccharides: all of the theories are correct. *Glycobiology* 3, 97-130.
7. Dwek, R. A. (1995) Glycobiology: "towards understanding the function of sugars". *Biochem Soc Trans* 23, 1-25.
8. Saxon, E., and Bertozzi, C. R. (2001) Chemical and biological strategies for engineering cell surface glycosylation. *Annu Rev Cell Dev Biol* 17, 1-23.
9. Isaji, T., Sato, Y., Zhao, Y., Miyoshi, E., Wada, Y., Taniguchi, N., and Gu, J. (2006) N-glycosylation of the beta-propeller domain of the integrin alpha5 subunit is essential for alpha5beta1 heterodimerization, expression on the cell surface, and its biological function. *J Biol Chem* 281, 33258-33267.
10. Isaji, T., Sato, Y., Fukuda, T., and Gu, J. (2009) N-glycosylation of the I-like domain of beta1 integrin is essential for beta1 integrin expression and biological function: identification of the minimal N-glycosylation requirement for alpha5beta1. *J Biol Chem* 284, 12207-12216.
11. Nicolaou, N., Margadant, C., Kevelam, S. H., Lilien, M. R., Oosterveld, M. J., Kreft, M., van Eerde, A. M., Pfundt, R., Terhal, P. A., van der Zwaag, B., Nikkels, P. G., Sachs, N., Goldschmeding, R., Knoers, N. V., Renkema, K. Y., and Sonnenberg, A. (2012) Gain of glycosylation in integrin alpha3 causes lung disease and nephrotic syndrome. *J Clin Invest* 122, 4375-4387.
12. Yoshimura, M., Ihara, Y., Matsuzawa, Y., and Taniguchi, N. (1996) Aberrant glycosylation of E-cadherin enhances cell-cell binding to suppress metastasis. *J Biol Chem* 271, 13811-13815.
13. Gu, J., and Taniguchi, N. (2008) Potential of N-glycan in cell adhesion and migration as either a positive or negative regulator. *Cell Adh Migr* 2, 243-245.
14. Guo, H. B., Johnson, H., Randolph, M., and Pierce, M. (2009) Regulation of homotypic cell-cell adhesion by branched N-glycosylation of N-cadherin extracellular EC2 and EC3 domains. *J Biol Chem* 284, 34986-34997.
15. Kannagi, R., Izawa, M., Koike, T., Miyazaki, K., and Kimura, N. (2004) Carbohydrate-mediated cell adhesion in cancer metastasis and angiogenesis. *Cancer Sci* 95, 377-384.
16. Izawa, M., Kumamoto, K., Mitsuoka, C., Kanamori, C., Kanamori, A., Ohmori, K., Ishida, H., Nakamura, S., Kurata-Miura, K., Sasaki, K., Nishi, T., and Kannagi, R. (2000)

Expression of sialyl 6-sulfo Lewis X is inversely correlated with conventional sialyl Lewis X expression in human colorectal cancer. *Cancer Res* 60, 1410-1416.
17. Kim, Y. J., and Varki, A. (1997) Perspectives on the significance of altered glycosylation of glycoproteins in cancer. *Glycoconj J* 14, 569-576.
18. Vogt, G., Chapgier, A., Yang, K., Chuzhanova, N., Feinberg, J., Fieschi, C., Boisson-Dupuis, S., Alcais, A., Filipe-Santos, O., Bustamante, J., de Beaucoudrey, L., Al-Mohsen, I., Al-Hajjar, S., Al-Ghonaium, A., Adimi, P., Mirsaeidi, M., Khalilzadeh, S., Rosenzweig, S., de la Calle Martin, O., Bauer, T. R., Puck, J. M., Ochs, H. D., Furthner, D., Engelhorn, C., Belohradsky, B., Mansouri, D., Holland, S. M., Schreiber, R. D., Abel, L., Cooper, D. N., Soudais, C., and Casanova, J. L. (2005) Gains of glycosylation comprise an unexpectedly large group of pathogenic mutations. *Nat Genet* 37, 692-700.
19. Woodhouse, E. C., Chuaqui, R. F., and Liotta, L. A. (1997) General mechanisms of metastasis. *Cancer* 80, 1529-1537.
20. Huttenlocher, A., and Horwitz, A. R. (2011) Integrins in cell migration. *Cold Spring Harb Perspect Biol* 3, a005074.
21. Chammas, R., Veiga, S. S., Line, S., Potocnjak, P., and Brentani, R. R. (1991) Asn-linked oligosaccharide-dependent interaction between laminin and gp120/140. An alpha 6/beta 1 integrin. *J Biol Chem* 266, 3349-3355.
22. Zheng, M., Fang, H., and Hakomori, S. (1994) Functional role of N-glycosylation in alpha 5 beta 1 integrin receptor. De-N-glycosylation induces dissociation or altered association of alpha 5 and beta 1 subunits and concomitant loss of fibronectin binding activity. *J Biol Chem* 269, 12325-12331.
23. Gu, J., and Taniguchi, N. (2004) Regulation of integrin functions by N-glycans. *Glycoconj J* 21, 9-15.
24. Bellis, S. L. (2004) Variant glycosylation: an underappreciated regulatory mechanism for beta1 integrins. *Biochim Biophys Acta* 1663, 52-60.
25. Miyoshi, E., Noda, K., Ko, J. H., Ekuni, A., Kitada, T., Uozumi, N., Ikeda, Y., Matsuura, N., Sasaki, Y., Hayashi, N., Hori, M., and Taniguchi, N. (1999) Overexpression of alpha1-6 fucosyltransferase in hepatoma cells suppresses intrahepatic metastasis after splenic injection in athymic mice. *Cancer Res* 59, 2237-2243.
26. Leitinger, B., and Hohenester, E. (2007) Mammalian collagen receptors. *Matrix Biol* 26, 146-155.
27. Arimoto-Ishida, E., Sakata, M., Sawada, K., Nakayama, M., Nishimoto, F., Mabuchi, S., Takeda, T., Yamamoto, T., Isobe, A., Okamoto, Y., Lengyel, E., Suehara, N., Morishige, K., and Kimura, T. (2009) Up-regulation of alpha5-integrin by E-cadherin loss in hypoxia and its key role in the migration of extravillous trophoblast cells during early implantation. *Endocrinology* 150, 4306-4315.
28. Ryu, M. H., Park, H. M., Chung, J., Lee, C. H., and Park, H. R. (2010) Hypoxia-inducible factor-1alpha mediates oral squamous cell carcinoma invasion via upregulation of alpha5 integrin and fibronectin. *Biochem Biophys Res Commun* 393, 11-15.
29. Weitzman, J. B., Pasqualini, R., Takada, Y., and Hemler, M. E. (1993) The function and distinctive regulation of the integrin VLA-3 in cell adhesion, spreading, and homotypic cell aggregation. *J Biol Chem* 268, 8651-8657.
30. Elices, M. J., Urry, L. A., and Hemler, M. E. (1991) Receptor functions for the integrin VLA-3: fibronectin, collagen, and laminin binding are differentially influenced by Arg-Gly-Asp peptide and by divalent cations. *J Cell Biol* 112, 169-181.

31. Dedhar, S., Jewell, K., Rojiani, M., and Gray, V. (1992) The receptor for the basement membrane glycoprotein entactin is the integrin alpha 3/beta 1. *J Biol Chem* 267, 18908-18914.
32. Carter, W. G., Ryan, M. C., and Gahr, P. J. (1991) Epiligrin, a new cell adhesion ligand for integrin alpha 3 beta 1 in epithelial basement membranes. *Cell* 65, 599-610.
33. Delwel, G. O., de Melker, A. A., Hogervorst, F., Jaspars, L. H., Fles, D. L., Kuikman, I., Lindblom, A., Paulsson, M., Timpl, R., and Sonnenberg, A. (1994) Distinct and overlapping ligand specificities of the alpha 3A beta 1 and alpha 6A beta 1 integrins: recognition of laminin isoforms. *Mol Biol Cell* 5, 203-215.
34. Guo, N., Templeton, N. S., Al-Barazi, H., Cashel, J. A., Sipes, J. M., Krutzsch, H. C., and Roberts, D. D. (2000) Thrombospondin-1 promotes alpha3beta1 integrin-mediated adhesion and neurite-like outgrowth and inhibits proliferation of small cell lung carcinoma cells. *Cancer Res* 60, 457-466.
35. Kreidberg, J. A. (2000) Functions of alpha3beta1 integrin. *Curr Opin Cell Biol* 12, 548-553.
36. Pignatelli, M., Hanby, A. M., and Stamp, G. W. (1991) Low expression of beta 1, alpha 2 and alpha 3 subunits of VLA integrins in malignant mammary tumours. *J Pathol* 165, 25-32.
37. Adachi, M., Taki, T., Huang, C., Higashiyama, M., Doi, O., Tsuji, T., and Miyake, M. (1998) Reduced integrin alpha3 expression as a factor of poor prognosis of patients with adenocarcinoma of the lung. *J Clin Oncol* 16, 1060-1067.
38. Barr, L. F., Campbell, S. E., Bochner, B. S., and Dang, C. V. (1998) Association of the decreased expression of alpha3beta1 integrin with the altered cell: environmental interactions and enhanced soft agar cloning ability of c-myc-overexpressing small cell lung cancer cells. *Cancer Res* 58, 5537-5545.
39. Judware, R., and Culp, L. A. (1997) Concomitant down-regulation of expression of integrin subunits by N-myc in human neuroblastoma cells: differential regulation of alpha2, alpha3 and beta1. *Oncogene* 14, 1341-1350.
40. Plopper, G. E., Domanico, S. Z., Cirulli, V., Kiosses, W. B., and Quaranta, V. (1998) Migration of breast epithelial cells on Laminin-5: differential role of integrins in normal and transformed cell types. *Breast Cancer Res Treat* 51, 57-69.
41. Ura, H., Denno, R., Hirata, K., Yamaguchi, K., and Yasoshima, T. (1998) Separate functions of alpha2beta1 and alpha3beta1 integrins in the metastatic process of human gastric carcinoma. *Surg Today* 28, 1001-1006.
42. Morelle, W., Canis, K., Chirat, F., Faid, V., and Michalski, J. C. (2006) The use of mass spectrometry for the proteomic analysis of glycosylation. *Proteomics* 6, 3993-4015.
43. Pan, S., Chen, R., Aebersold, R., and Brentnall, T. A. (2011) Mass spectrometry based glycoproteomics--from a proteomics perspective. *Mol Cell Proteomics* 10, R110 003251.
44. Madera, M., Mechref, Y., and Novotny, M. V. (2005) Combining lectin microcolumns with high-resolution separation techniques for enrichment of glycoproteins and glycopeptides. *Anal Chem* 77, 4081-4090.
45. Ongay, S., Boichenko, A., Govorukhina, N., and Bischoff, R. (2012) Glycopeptide enrichment and separation for protein glycosylation analysis. *J Sep Sci* 35, 2341-2372.
46. Zhang, H., Li, X. J., Martin, D. B., and Aebersold, R. (2003) Identification and quantification of N-linked glycoproteins using hydrazide chemistry, stable isotope labeling and mass spectrometry. *Nat Biotechnol* 21, 660-666.

47. Lewandrowski, U., Zahedi, R. P., Moebius, J., Walter, U., and Sickmann, A. (2007) Enhanced N-glycosylation site analysis of sialoglycopeptides by strong cation exchange prefractionation applied to platelet plasma membranes. *Mol Cell Proteomics* 6, 1933-1941.
48. Alpert, A. J. (1990) Hydrophilic-interaction chromatography for the separation of peptides, nucleic acids and other polar compounds. *J Chromatogr* 499, 177-196.
49. Larsen, M. R., Jensen, S. S., Jakobsen, L. A., and Heegaard, N. H. (2007) Exploring the sialiome using titanium dioxide chromatography and mass spectrometry. *Mol Cell Proteomics* 6, 1778-1787.
50. Lei, Z., Beuerman, R. W., Chew, A. P., Koh, S. K., Cafaro, T. A., Urrets-Zavalia, E. A., Urrets-Zavalia, J. A., Li, S. F., and Serra, H. M. (2009) Quantitative analysis of N-linked glycoproteins in tear fluid of climatic droplet keratopathy by glycopeptide capture and iTRAQ. *J Proteome Res* 8, 1992-2003.
51. Palmisano, G., Parker, B. L., Engholm-Keller, K., Lendal, S. E., Kulej, K., Schulz, M., Schwammle, V., Graham, M. E., Saxtorph, H., Cordwell, S. J., and Larsen, M. R. (2012) A novel method for the simultaneous enrichment, identification, and quantification of phosphopeptides and sialylated glycopeptides applied to a temporal profile of mouse brain development. *Mol Cell Proteomics* 11, 1191-1202.
52. Hao, P., Guo, T., and Sze, S. K. (2011) Simultaneous analysis of proteome, phospho- and glycoproteome of rat kidney tissue with electrostatic repulsion hydrophilic interaction chromatography. *PLoS One* 6, e16884.
53. Zhang, H., Guo, T., Li, X., Datta, A., Park, J. E., Yang, J., Lim, S. K., Tam, J. P., and Sze, S. K. (2010) Simultaneous characterization of glyco- and phosphoproteomes of mouse brain membrane proteome with electrostatic repulsion hydrophilic interaction chromatography. *Mol Cell Proteomics* 9, 635-647.
54. Alpert, A. J. (2008) Electrostatic repulsion hydrophilic interaction chromatography for isocratic separation of charged solutes and selective isolation of phosphopeptides. *Anal Chem* 80, 62-76.
55. Hao, P., Qian, J., Ren, Y., and Sze, S. K. (2011) Electrostatic repulsion-hydrophilic interaction chromatography (ERLIC) versus strong cation exchange (SCX) for fractionation of iTRAQ-labeled peptides. *J Proteome Res* 10, 5568-5574.
56. Hao, P., Ren, Y., Alpert, A. J., and Sze, S. K. (2011) Detection, evaluation and minimization of nonenzymatic deamidation in proteomic sample preparation. *Mol Cell Proteomics* 10, O111 009381.
57. Wright, H. T. (1991) Sequence and structure determinants of the nonenzymatic deamidation of asparagine and glutamine residues in proteins. *Protein Eng* 4, 283-294.
58. Huang da, W., Sherman, B. T., and Lempicki, R. A. (2009) Systematic and integrative analysis of large gene lists using DAVID bioinformatics resources. *Nat Protoc* 4, 44-57.
59. Parker, B. L., Palmisano, G., Edwards, A. V., White, M. Y., Engholm-Keller, K., Lee, A., Scott, N. E., Kolarich, D., Hambly, B. D., Packer, N. H., Larsen, M. R., and Cordwell, S. J. (2011) Quantitative N-linked glycoproteomics of myocardial ischemia and reperfusion injury reveals early remodeling in the extracellular environment. *Mol Cell Proteomics* 10, M110 006833.
60. Hemler, M. E., Huang, C., and Schwarz, L. (1987) The VLA protein family. Characterization of five distinct cell surface heterodimers each with a common 130,000 molecular weight beta subunit. *J Biol Chem* 262, 3300-3309.

61. Takada, Y., Huang, C., and Hemler, M. E. (1987) Fibronectin receptor structures in the VLA family of heterodimers. *Nature* 326, 607-609.
62. Nguyen, B. P., Ryan, M. C., Gil, S. G., and Carter, W. G. (2000) Deposition of laminin 5 in epidermal wounds regulates integrin signaling and adhesion. *Curr Opin Cell Biol* 12, 554-562.
63. Zhou, H., and Kramer, R. H. (2005) Integrin engagement differentially modulates epithelial cell motility by RhoA/ROCK and PAK1. *J Biol Chem* 280, 10624-10635.
64. Goldfinger, L. E., Hopkinson, S. B., deHart, G. W., Collawn, S., Couchman, J. R., and Jones, J. C. (1999) The alpha3 laminin subunit, alpha6beta4 and alpha3beta1 integrin coordinately regulate wound healing in cultured epithelial cells and in the skin. *J Cell Sci* 112 (Pt 16), 2615-2629.
65. Wen, T., Zhang, Z., Yu, Y., Qu, H., Koch, M., and Aumailley, M. (2010) Integrin alpha3 subunit regulates events linked to epithelial repair, including keratinocyte migration and protein expression. *Wound Repair Regen* 18, 325-334.
66. Mitchell, K., Svenson, K. B., Longmate, W. M., Gkirtzimanaki, K., Sadej, R., Wang, X., Zhao, J., Eliopoulos, A. G., Berditchevski, F., and Dipersio, C. M. (2010) Suppression of integrin alpha3beta1 in breast cancer cells reduces cyclooxygenase-2 gene expression and inhibits tumorigenesis, invasion, and cross-talk to endothelial cells. *Cancer Res* 70, 6359-6367.

Figure Legends

Figure 1. Experimental workflow for iTRAQ analysis of N-linked glycoprotein from A431 cells.

Figure 2. The glycosylation of integrin subunits were modulated by hypoxia. A) Panther pathway analysis result for all identified putative glycoproteins; B) iTRAQ analysis result for identified glycopeptide changes of 5 integrin subunits modulated by hypoxia; C) iTRAQ analysis result for the changes of three identified glycopeptides in ITGA3 responsible for hypoxia;

Figure 3. Less ITGA3 is detected on the plasma membrane of A431 cells under hypoxia. WB results showed that only the higher MW isoform of ITGA3 was down-regulated by hypoxia (A), which disappeared and combined with smaller isoform as one band with lower MW after N-glycan removal (B), and this decrease was amplified in the membrane fractions (Lowest panel in panel A). Lower levels of membrane ITGA3 on A431 cells under hypoxia were confirmed by flow cytometry (C) and immunofluorescence cell statining(D).

Figure 4. N-linked glycosylation sites 6 and 7 were essential for the translocation of ITGA3 to the plasma membrane in K562 cells. A) WB revealed a single ITGA3 band in K562-M6-7 mutants, with an absence of ITGA3 in membrane or biotinlytion fractions. Accordingly no binding of ITGA3 and ITGB1 was detected in IP experiments. B) Transfection of WT ITGA3 into K562 cells rescued cell spreading on laminin 5, while no cell spreading was detected in cells expressing M6-7. Arrows indicate spread cells on laminin 5-coated plates.

Figure 5. A431-M6-7 cells with less membrane ITGA3 had more invasive ability than A431-WT under hypoxia. A) and B) The whole or membrane ITGA3 in the stable cell lines transfected with blank plasmids (control), WT, M6-7 or M3-5 ITGA3 was detected by WB and flow cytometry respectively; C) and D) Transwell images for each stable cell line under normoxia for 24h and hypoxia for 24h, respectively. E) and F) Transwell quantification results for each stable cell line under Nx and Hx measured by crystal violet OD_{595}. For normoxia, 0.5μg/ml laminin 5 was coated with transwell membranes and the medium with 5% FBS was added into the lower chambers. For hypoxia, to improve invasion, 1μg/ml laminin 5 was coated with transwell membranes. 2.5% FBS and 10% FBS in the medium were adopted for cell suspension in the upper inserts and cell migratory stimulus in the lower chambers, respectively. The plates were subjected to normoxia for 2 hours for cell attachment after cell seeded, and then put into hypoxia chambers.

Tables and Figures

Table 1, Analysis of glycoproteins isolated by ERLIC enrichment and Q-Star Elite identification

Glycoprotein No.	Glycopeptide No.	Glycosite No.	Glycosite Characterization		
			With Reference support	Potential	Unknown
146	241*	215	93	50	72

*All glycopeptides have ≥95% identification confidence and one site might be repeatedly identified in different peptides.

Figure 1

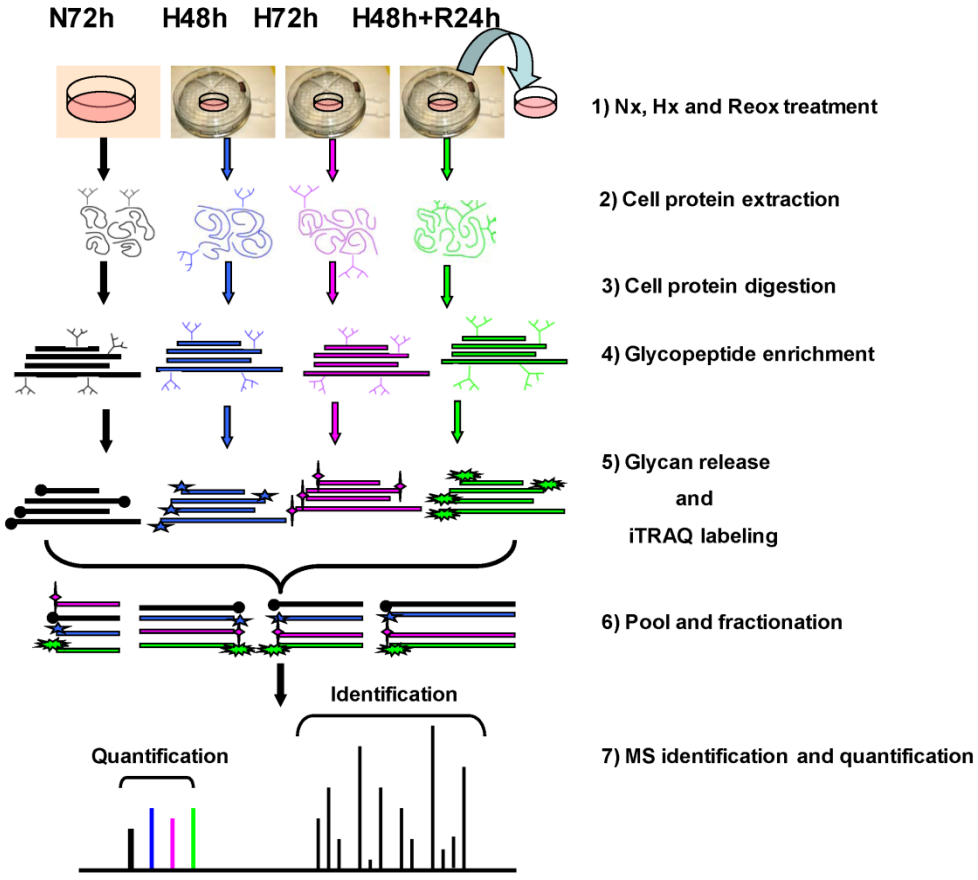
N72h
H48h
H72h
H48h+R24h
1) Nx, Hx and Reox treatment
2) Cell protein extraction
3) Cell protein digestion
4) Glycopeptide enrichment
5) Glycan release
and
iTRAQ labeling
6) Pool and fractionation
Identification
Quantification
7) MS identification and quantification

Figure 2

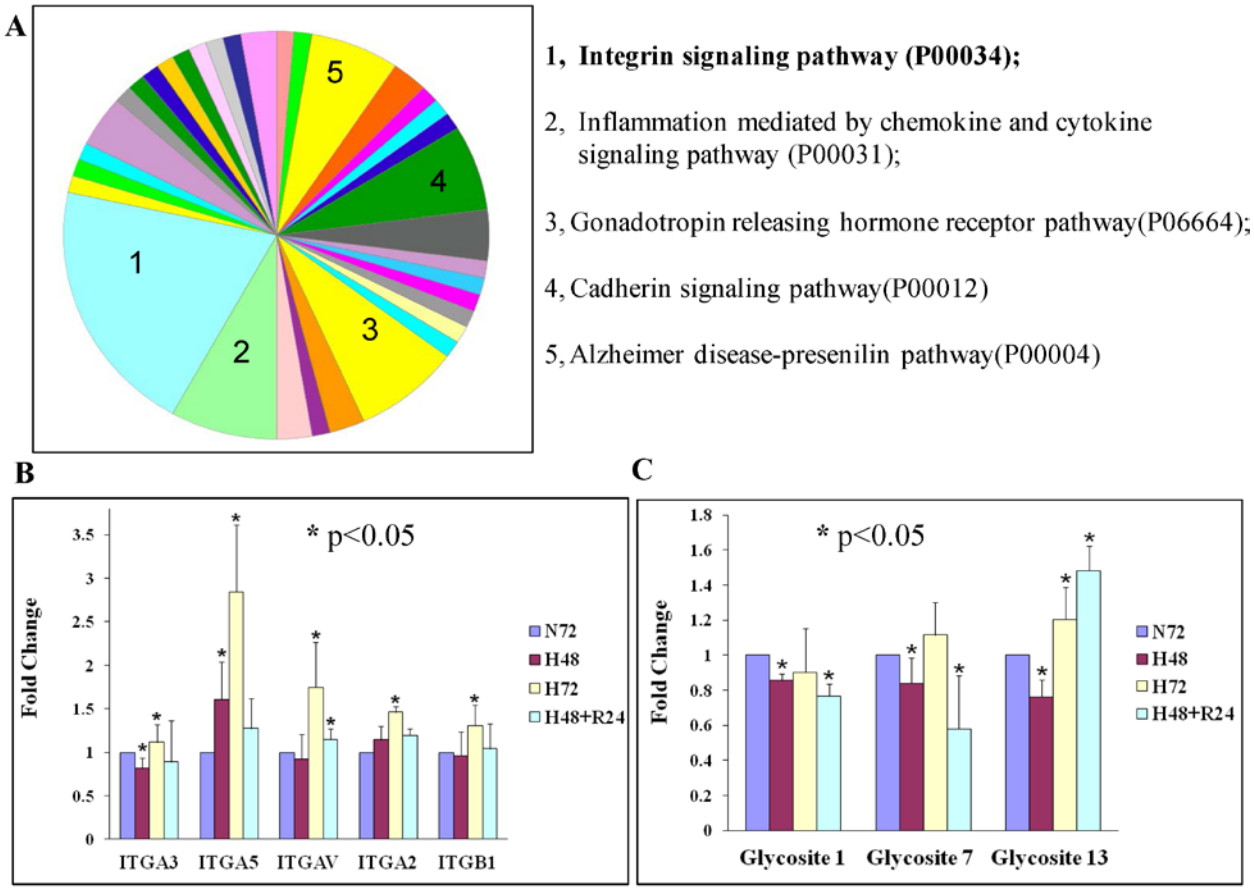
A
1
2
3
4
5
1, Integrin signaling pathway (P00034);
2, Inflammation mediated by chemokine and cytokine signaling pathway (P00031);
3, Gonadotropin releasing hormone receptor pathway(P06664);
4, Cadherin signaling pathway(P00012)
5, Alzheimer disease-presenilin pathway(P00004)
B
* p<0.05
Fold Change
ITGA3
ITGA5
ITGAV
ITGA2
ITGB1
N72
H48
H72
H48+R24
C
* p<0.05
Fold Change
Glycosite 1
Glycosite 7
Glycosite 13
N72
H48
H72
H48+R24

Figure 3

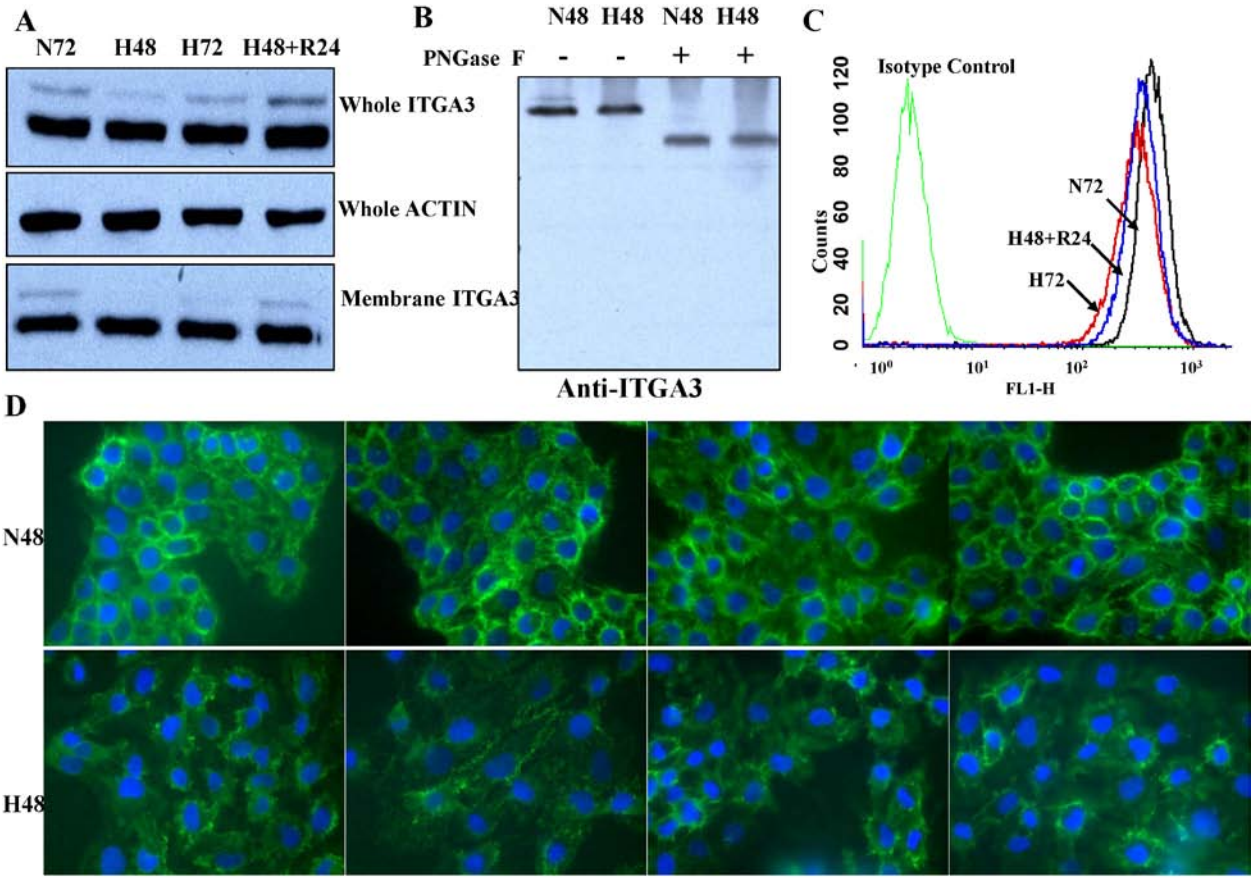
A
N72
H48
H72
H48+R24
Whole ITGA3
Whole ACTIN
Membrane ITGA3
B
N48 H48 N48 H48
PNGase F - - + +
Anti-ITGA3
C
Isotype Control
N72
H48+R24
H72
Counts
FL1-H
D
N48
H48

Figure 4

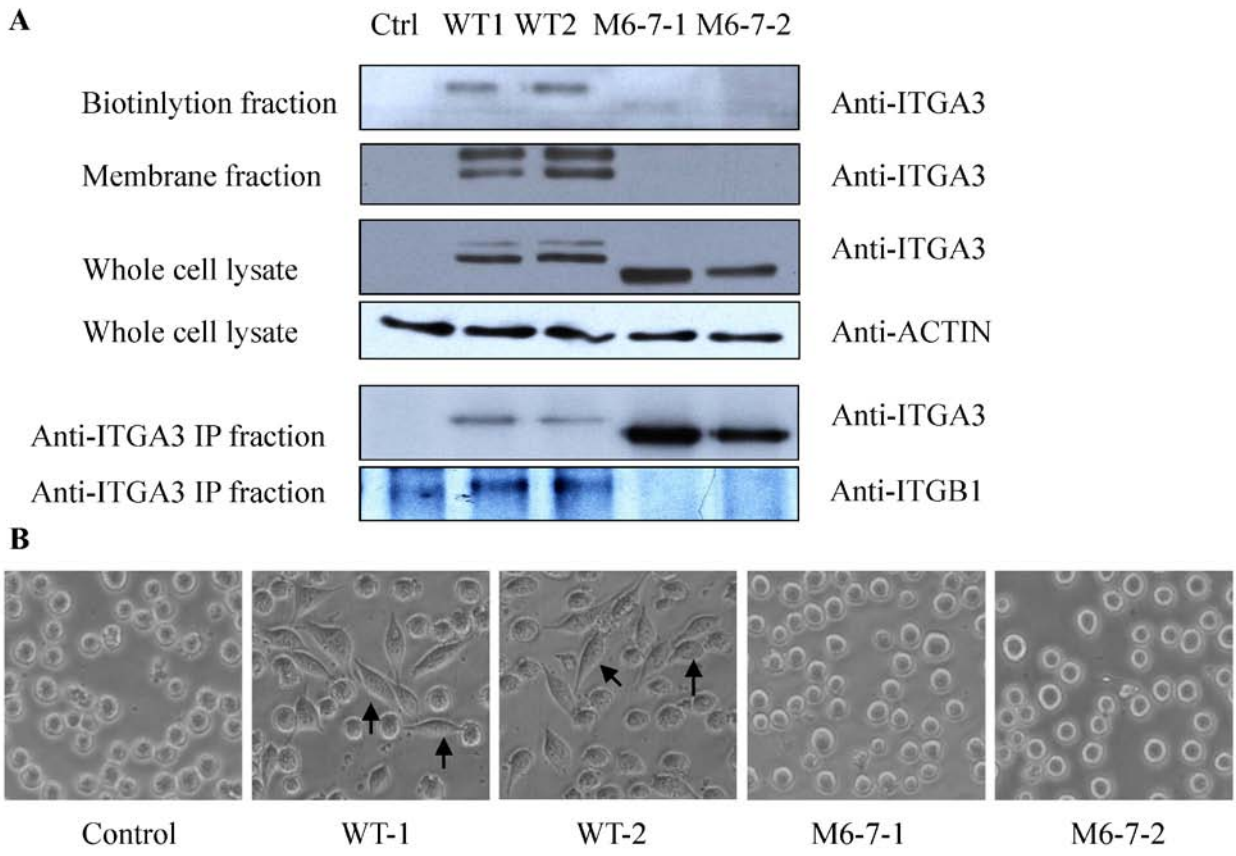
A
Ctrl WT1 WT2 M6-7-1 M6-7-2
Biotinlytion fraction
Anti-ITGA3
Membrane fraction
Anti-ITGA3
Whole cell lysate
Anti-ITGA3
Whole cell lysate
Anti-ACTIN
Anti-ITGA3 IP fraction
Anti-ITGA3
Anti-ITGA3 IP fraction
Anti-ITGB1
B
Control
WT-1
WT-2
M6-7-1
M6-7-2

Figure 5

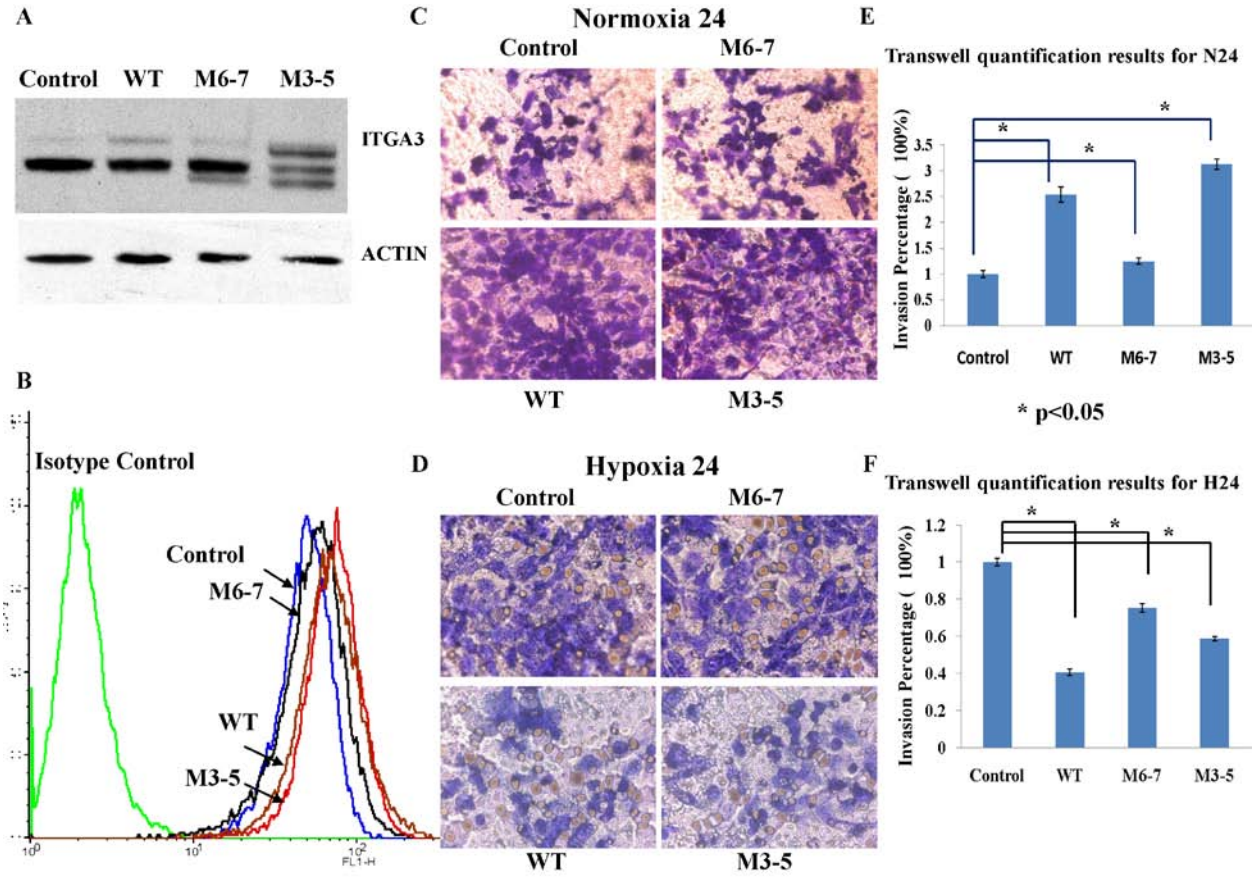
A
Control
WT
M6-7
M3-5
ITGA3
ACTIN
B
Isotype Control
Control
M6-7
WT
M3-5
FL1-H
C
Normoxia 24
Control
M6-7
WT
M3-5
D
Hypoxia 24
Control
M6-7
WT
M3-5
E
Transwell quantification results for N24
Invasion Percentage (100%)
Control
WT
M6-7
M3-5
* p<0.05
F
Transwell quantification results for H24
Invasion Percentage (100%)
Control
WT
M6-7
M3-5